Published OnlineFirst September 30, 2010; DOI: 10.1158/0008-5472.CAN-10-1825

Microenvironment and Immunology

Cancer Research

Improved Clinical Outcome in Indolent B-Cell Lymphoma Patients Vaccinated with Autologous Tumor Cells Experiencing Immunogenic Death

Roberta Zappasodi[1], Serenella M. Pupa[2], Gaia C. Ghedini[2], Italia Bongarzone[3], Michele Magni[1], Antonello D. Cabras[4], Mario P. Colombo[5], Carmelo Carlo-Stella[1,6], Alessandro M. Gianni[1,6], and Massimo Di Nicola[1]

Abstract

Increasing evidence argues that the success of an anticancer treatment may rely on immunoadjuvant side effects including the induction of immunogenic tumor cell death. Based on the assumption that this death mechanism is a similar prerequisite for the efficacy of an active immunotherapy using killed tumor cells, we examined a vaccination strategy using dendritic cells (DC) loaded with apoptotic and necrotic cell bodies derived from autologous tumors. Using this approach, clinical and immunologic responses were achieved in 6 of 18 patients with relapsed indolent non–Hodgkin's lymphoma (NHL). The present report illustrates an impaired ability of the neoplastic cells used to vaccinate nonresponders to undergo immunogenic death on exposure to a cell death protocol based on heat shock, γ-ray, and UVC ray. Interestingly, when compared with doxorubicin, this treatment increased surface translocation of calreticulin and cellular release of high-mobility group box 1 and ATP in histologically distinct NHL cell lines. In contrast, treated lymphoma cells from responders displayed higher amounts of calreticulin and heat shock protein 90 (HSP90) compared with those from nonresponders and boosted the production of specific antibodies when loaded into DCs for vaccination. Accordingly, the extent of calreticulin and HSP90 surface expression in the DC antigenic cargo was significantly associated with the clinical and immunologic responses achieved. Our results indicate that a positive clinical effect is obtained when immunogenically killed autologous neoplastic cells are used for the generation of a DC-based vaccine. Therapeutic improvements may thus be accomplished by circumventing the tumor-impaired ability to undergo immunogenic death and prime the antitumor immune response. *Cancer Res; 70(22); 9062–72. ©2010 AACR.*

Introduction

Vaccination with cancer cells treated *ex vivo* with antracyclines or oxaliplatin or ionizing radiation protects mice against a subsequent challenge with live tumor cells (1–4). The immunizing properties of killed tumor cells depends on the ability of a cytotoxic agent to render their death immunogenic so that the immune system can be specifically alerted to the presence of a tumor (5). Similarly, the way in which neoplastic cells are killed to produce the antigenic content of a dendritic cell (DC)–based vaccine may be crucial for priming a clinically efficacious antitumor immune response. We recently reported that vaccination with autologous monocyte-derived DCs pulsed with autologous tumor cells dying after exposure to heat shock (HS), γ-ray, and UVC ray elicited a clinical response associated with tumor-specific immune activation in 6 of 18 relapsed indolent non–Hodgkin's lymphoma (NHL) patients (6). We have now sought to determine whether responders and nonresponders can be distinguished in terms of immunogenic tumor cell killing at the time of vaccine preparation. Preclinical studies of radio/chemotherapy-elicited immunogenic cell death in sarcoma, breast, and colon carcinoma mouse models (1, 3, 7) have shown that the release of "eat-me" and danger signals by tumor cells is the main molecular mechanism whereby DC engulfment of dead cell particles and their activation promote the cross-priming of tumor antigens and induction of a specific adaptive immune response (8, 9). Immunogenic cell death is preceded by relocation of the endoplasmic reticulum-resident chaperone calreticulin (CRT; refs. 1, 10, 11) to the plasma membrane, followed by surface expressions of HS protein 70 (HSP70) and HSP90 (12) that act as vehicles

Authors' Affiliations: [1]C. Gandini Medical Oncology, Bone Marrow Transplantation Unit, [2]Molecular Targeting Unit, [3]Proteomics Laboratory, Department of Experimental Oncology, [4]Pathology Unit, and [5]Immunotherapy and Gene Therapy Unit, Department of Experimental Oncology, Fondazione Istituti di Ricovero e Cura a Carattere Scientifico, Istituto Nazionale per lo Studio e la Cura dei Tumori; and [6]School of Medical Oncology, University of Milan, Milan, Italy

Note: Supplementary data for this article are available at Cancer Research Online (http://cancerres.aacrjournals.org/).

R. Zappasodi and S.M. Pupa contributed equally to this work.

Corresponding Author: Massimo Di Nicola, C. Gandini Medical Oncology, Bone Marrow Transplantation Unit, Istituto Nazionale per lo Studio e la Cura dei Tumori, Via Venezian 1, 20133 Milan, Italy. Phone: 39-2-239-2506; Fax: 39-2-239-3461; E-mail: massimo.dinicola@istitutotumori.mi.it.

doi: 10.1158/0008-5472.CAN-10-1825

Published OnlineFirst September 30, 2010; DOI: 10.1158/0008-5472.CAN-10-1825

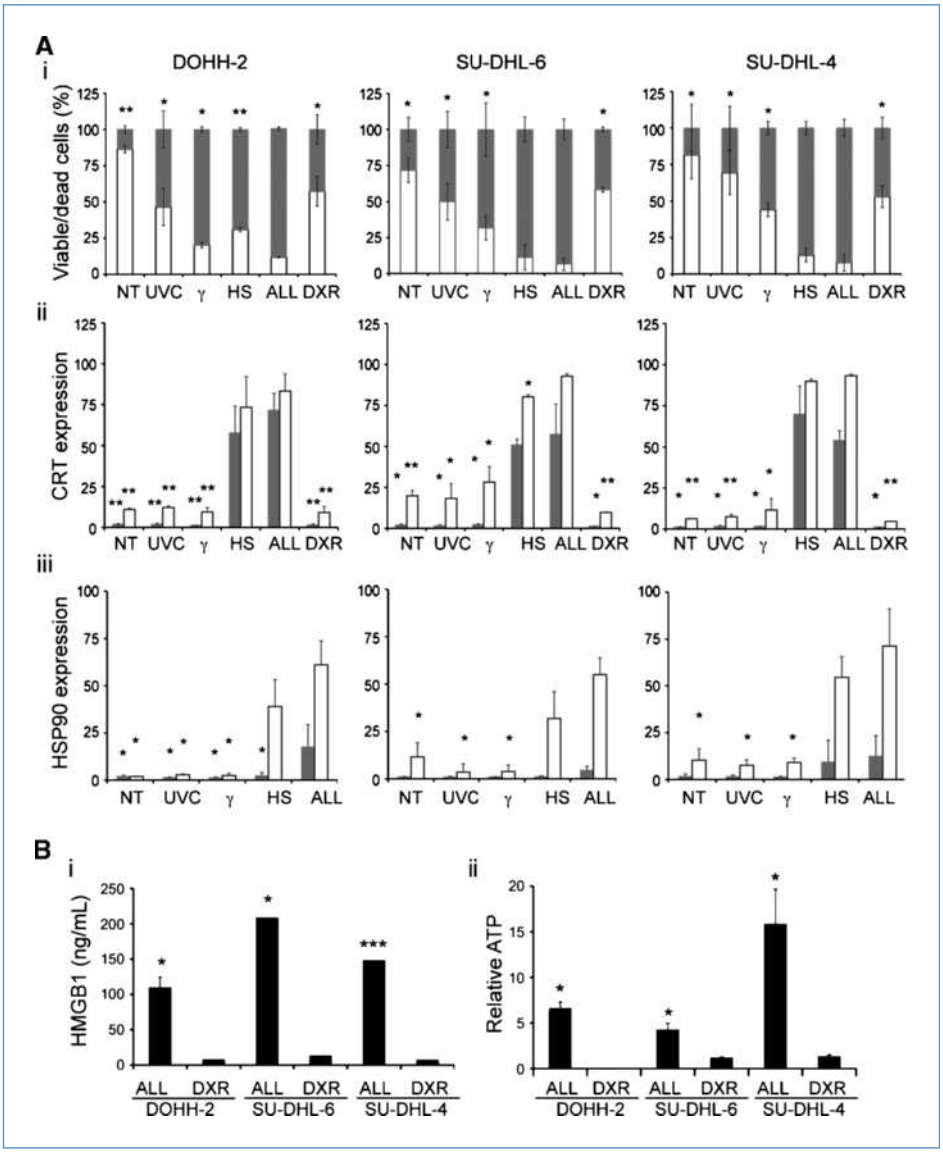

Figure 1. Immunogenic cell death in NHL cell lines. Twenty-four hours following exposure to DXR or UVC, γ irradiation, and HS as single or associated (ALL) treatments, the ability of NHL cell lines to undergo immunogenic death was assessed. Nontreated cultures (NT) were included as control. A, percentage of viable (white) and dead cells (gray) as determined by trypan blue exclusion test (i); flow cytometry analyses of CRT (ii) and HSP90 (iii) relative MFI (gray columns) and positive cell frequency (white columns). Relative MFI was calculated as the ratio between stained sample and negative control MFI. Analyses were performed on 7-AAD–negative gated events. Left, middle, and right, results obtained with DOHH-2, SU-DHL-6, and SU-DHL-4 cell lines, respectively. B, quantification of HMGB1 (i) and ATP (ii) in culture supernatant. For each cell line, ATP release was normalized by the amount found in untreated cultures, giving relative ATP values. Statistically significant differences between ALL and the other culture conditions were calculated using the two-sided Student's *t* test (*, $P \leq 0.05$; **, $P \leq 0.001$; ***, $P \leq 0.0001$). The average values of results obtained in three independent experiments are reported.

for peptide antigens (13–15) or direct immunogenic signals for DC activation (16–19). Next, dying tumor cells release ATP (20, 21) and the nuclear factor high-mobility group box 1 (HMGB1; refs. 7, 22), both essential for DC activation and antigen presentation to specific cytotoxic T cells. We have assessed the ability of HS, γ-ray, and UVC ray to induce CRT and HSP translocation as well as HMGB1 and ATP release from three cell lines, representing low-, intermediate-, and high-grade NHL. We then compared these outcomes to the effect of doxorubicin (DXR), a well-recognized immunogenic cell death inducer (1, 2, 7, 20). The results show that our cell death protocol was even more efficient than DXR treatment in inducing the processes that define immunogenic cell death in all three NHL cell lines. As to the identification of predictors of the clinical outcome of a cancer vaccine (6), we speculated that defective exposure of immunogenic signals (10) by heat-shocked, γ-irradiated, and UVC-irradiated tumor cells used as antigenic cargo for a DC-based vaccine might be associated with a reduced probability of response. When primary indolent NHL was studied, in fact, observation of a difference in the ability of the tumor to undergo immunogenic cell death pointed to a critical association between the amount of immunogenic signals emitted by apoptotic and necrotic tumor cell bodies and the clinical efficacy of a DC-based vaccine.

Materials and Methods

Cell lines, primary cells, and culture conditions

DOHH-2, SU-DHL-6, and SU-DHL-4 cell lines, representing follicular centroblastic/centrocytic, diffuse mixed small- and large-cell, and diffuse large-cell cleaved cell NHL, respectively, were purchased from DSMZ and cultured in RPMI 1640 (Lonza) supplemented with 10% (v/v) inactivated fetal

Published OnlineFirst September 30, 2010; DOI: 10.1158/0008-5472.CAN-10-1825

Table 1. GO of proteins significantly represented in DOHH-2 apoptotic and necrotic bodies

GO terms	Fold enrichment	*P*
Endoplasmic reticulum	1.87	1.36E–002
Actin cytoskeleton organization	1.95	1.12E–002
HSP70	2.8	1.47E–003
Intracellular transport	3	1.05E–003
ATP carrier protein	3	1.02E–003
ATP biosynthesis	3.4	3.95E–004
UPR/stress response	3.7	1.70E–004
Localization/transport	4	9.31E–005
HSP90	4.1	7.38E–005
Catabolic processes	4.1	7.27E–005
ATP binding	4.6	2.20E–005
Monosaccharide metabolism	5	8.89E–006
Intracellular	5.9	1.24E–006
Vesicle	6.8	1.60E–008
Mitochondrion	12.6	2.61E–013

bovine serum (Lonza), 1% (v/v) L-glutamine (Lonza), and 1% (v/v) HEPES buffer (Lonza) in a humidified chamber (95% air, 5% CO_2) at 37°C. All cell lines were regularly screened to ensure the absence of *Mycoplasma* contamination by MycoAlert *Mycoplasma* detection kit (Lonza), according to the manufacturer's instructions. Primary lymphoma cells were isolated from lymph nodes or peripheral blood (PB) as previously reported (6). Written informed consent for the investigational use of lymphocytes, serum samples, and tumor specimens was obtained from each patient. Apoptotic and necrotic cell bodies were generated by exposing primary lymphoma cells and cell lines to HS, γ-irradiation (γ), and UVC rays (UVC) in accordance with a previously described cell death induction protocol (6, 23) called ALL in this article when compared with the same agents used singly. Lymphoma cells were also treated with DXR (Pfizer Italia s.r.l.) at the indicated doses as the positive control for immunogenic death induction.

Flow cytometry

Surface stainings were performed as described (24) after blocking nonspecific antibody binding to the Fc receptors (FcR blocking reagent, Miltenyi Biotec). The following mouse anti-human antibodies were used: monoclonal FITC-labeled anti-HLA-DQ, PerCP-labeled anti-HLA-DR (BD Biosciences), phycoerythrin (PE)-labeled anti-HSP70, anti-HSP90, purified anti-CRT (Stressgen), and polyclonal anti-HLA class I (clone W6/32, Sera-Lab). FITC-labeled goat anti-mouse immunoglobulins (Jackson Imunoresearch) formed the secondary antibody. To avoid intracellular protein detection, dead cells were excluded by 7-aminoactinomycin D (7-AAD; Invitrogen) costaining (1 μg/mL for 20 minutes at 4°C). The immunophenotypic analyses of regulatory T cells (Treg) and natural killer (NK) cells were determined as described (6) in prevaccination and postvaccination PB samples from the patients whose immunologic monitoring was not part of the previous study (6). As negative controls, cells were incubated in parallel with the proper isotype immunoglobulins (PE-labeled and purified mouse IgG1, Stressgen; FITC-labeled rat IgG2a, eBiosciences). Samples were acquired by setting photomultiplier tubes on the autofluorescence of the related negative control. All plots were gated on high forward scatter (FSC) and low side scatter (SSC) to exclude cell debris. A minimum of 50,000 gated events was collected per sample. The apoptosis detection kit (Bender MedSystem) was used in accordance with the manufacturer's protocol. Data were acquired on a BD FACSCalibur using BD CellQuest software version 3.3 (Becton Dickinson) and analyzed by FlowJo 8.7.1 software version for Macintosh (Tree Star, Inc.).

ELISA

Cellular release of HMGB1 was measured in 24-hour culture supernatants using the appropriate ELISA kit according to the manufacturer's instructions (Shino Test Corporation).

ATP release assay

Extracellular ATP was measured in 24-hour culture supernatants by means of the luciferin-based ENLITEN ATP Assay (Promega). Light emission was recorded with a Berthold luminometer (Berthold Detection Systems Gmbh).

Table 2. KEGG pathways significantly represented by ALL-treated DOHH-2 cells

KEGG pathway	%	Fold enrichment	*P*
hsa04810: regulation of actin cytoskeleton	10.53	2.9	4.99E–002
hsa00190: oxidative phosphorylation	12.28	5.6	1.15E–003
hsa04612: antigen processing and presentation	8.77	6.4	6.55E–003
hsa00010: glycolysis/gluconeogenesis	7.02	6.9	1.87E–002
hsa05040: Huntington's disease	5.26	10.6	3.04E–002
hsa00710: carbon fixation	5.26	13.4	1.96E–002
hsa00020: citrate cycle (TCA cycle)	7.02	13.7	2.69E–003

Published OnlineFirst September 30, 2010; DOI: 10.1158/0008-5472.CAN-10-1825

Purification and biotinylation of human immunoglobulins

Antibody purification from human serum and immunoglobulin biotinylation were performed as described (6).

Western blot

DOHH-2 cells or apoptotic and necrotic cell bodies were lysed for 1 hour on ice in lysis buffer [50 mmol/L Tris-HCl (pH 7.2), 150 mmol/L NaCl, 100 mmol/L NaF, 100 mmol/L sodium pyruvate, 1% Triton X-100] containing protease inhibitors, 2 mmol/L phenylmethylsulfonylfluoride, 10 μg/mL aprotinin, and 2 mmol/L Na3VO4. Protein extracts were separated by electrophoresis on precast polyacrylamide gels (Invitrogen), transferred to hydrophobic polyvinylidene difluoride membranes (Amersham), probed with biotinylated human immunoglobulins, anti-CRT, anti-HSP90, and anti-HSP70 (Stressgen) monoclonal antibodies or rabbit anti-human actin polyclonal antibody (Sigma), and visualized as previously described (25). Full-range rainbow molecular marker (12–225 kDa; Amersham) and sharp protein standard (3.5–260 kDa; Novex, Invitrogen) were run in parallel in each SDS-PAGE analyses.

In-gel tryptic digestion, matrix-assisted laser desorption/ionization–time-of-flight mass spectrometry analysis, and peptide mass fingerprinting

For protein profiling of DOHH-2 apoptotic and necrotic cell bodies, protein bands were excised from Coomassie-stained preparative gels and processed as previously described (26). Matrix-assisted laser desorption/ionization–time-of-flight mass spectrometry was carried out with a Voyager-DE STR (Applied Biosystems), equipped with a nitrogen laser (337 nm). Monoisotopic peptide masses were analyzed using Aldente software (http://www.expasy.ch/tools/aldente/). Input was searched according to the following database: Aldente, UniProtKB/SwissProt; predefined taxon, Mammalia; spectrometer internal error max, 25. Only proteins identified from three or more separate experiments were considered.

Gene Ontology analysis

The Database for Annotation, Visualization, and Integrated Discovery (http://david.abcc.ncifcrf.gov/) was used to discover the Gene Ontology (GO) biological processes, cellular components, and molecular functions (GO terms) and KEGG pathways significantly represented by proteins from DOHH-2 apoptotic and necrotic bodies.

Statistical analysis

Statistical significance was calculated using the two-sided Student's t test ($P \leq 0.05$). Pearson and Spearman correlation coefficients were calculated to measure dependence between variables. Statistical analyses were performed on the Prism 5.0a software version for Macintosh (GraphPad Software, Inc.).

Results

Immunogenic signals in heat-shocked, γ-irradiated, and UVC-irradiated NHL cell lines

The extent of CRT cell surface translocation, HMGB1, and ATP release were evaluated in DOHH-2, SU-DHL-6, and SU-DHL-4 cell lines treated with HS, γ, UVC, or ALL. Cells were treated with DXR in parallel as positive control. The extent of CRT cell surface translocation was directly proportional to the amount of DXR in a limited dose interval (0.1–20 μmol/L) and peaked at 0.5, 2.5, and 15 μmol/L for DOHH-2, SU-DHL-6, and SU-DHL-4, respectively (data not shown). DXR was therefore administered at 0.5, 2.5, and 15 μmol/L in cultures of DOHH-2, SU-DHL-6, and SU-DHL-4 cells, respectively, and ~50% cell growth inhibition was reached after 24 hours (Fig. 1A, i). ALL was highly cytotoxic against the three NHL cell lines tested, as shown by the trypan blue exclusion test and flow cytometry analysis of apoptosis (Fig. 1A, i; Supplementary Fig. S1A). ALL-treated cells expressed surface-CRT at a higher frequency (Fig. 1A, ii, white columns; Supplementary Fig. S2A for a representative example) and intensity (Fig. 1A, ii, gray columns; Supplementary Fig. S2A for a representative example) compared with cells exposed to γ, UVC, or DXR alone. ALL provided a similar amount of CRT cell surface translocation, regardless of lymphoma histologic grade (Fig. 1A, ii, left versus middle versus right; Supplementary Fig. S2A for a representative example). As additional signals promoting the recognition and uptake of dying cells by DCs, the surface expression of stress-inducible HSP90 and HSP70 was evaluated. ALL significantly enhanced that of HSP90 in DOHH-2, SU-DHL-6, or SU-DHL-4 compared with γ or UVC alone (Fig. 1A, iii; Supplementary Fig. S2B for a representative example), but that of HSP70 only in SU-DHL-6 cells and to a lesser extent (Supplementary Figs. S1B and S2C for a representative example). The ability of DXR and ALL to stimulate cellular release of HMGB1 and ATP, two distinctive signals of immunogenic cell death, was also compared. For each cell line tested, ALL provided a significantly higher release of HMGB1 and ATP from each cell line than DXR administration as revealed by specific ELISA and luciferin-based assays in 24-hour conditioned culture media (Fig. 1B, i, $P = 0.045$, $P = 0.029$, $P = 0.0002$ and ii, $P = 0.049$, $P = 0.045$, $P = 0.024$). Interestingly, CRT and HSP90 exposure in heat-shocked NHL cell lines was comparable with that achieved in ALL-treated cells (Fig. 1A, ii and iii); however, HS alone was less efficient than ALL to boost ATP and HMGB1 release from all three cell lines (data not shown). Combination of γ and UVC with HS was thus a harmful way of inducing all reported mediators of immunogenic cell death in the three differently aggressive NHL cell lines. Coomassie staining revealed that ALL deeply modified the DOHH-2 cell protein pattern (Supplementary Fig. S3A and B). Mass spectrometry–based multiplexed profiling of apoptotic/necrotic DOHH-2 cell bodies highlighted an enrichment in proteins involved in mitochondrion and endoplasmic reticulum functions, ATP metabolism, intracellular organelle reorganization, and stress response, which are represented in 15 GO categories (Table 1; Supplementary Table S1). Seven KEGG pathways, including oxidative phosphorylation, citrate cycle, and antigen processing and presentation, were also significantly represented in ALL-treated DOHH-2 cells (Table 2). Most of the functions and pathways detected were integrally involved in apoptosis and in biochemical events associated with the immunogenicity of dying

Published OnlineFirst September 30, 2010; DOI: 10.1158/0008-5472.CAN-10-1825

Table 3. Clinical and immunologic characteristics of vaccinated patients

UPN no.	Age/sex	NHL type, stage	Previous treatment (response/duration)	Clinical response (length in mo)
12	65/M	LP, Stage IA	6 CVP (CR/36 mo)	CR (67)
13	72/F	FL grade I, Stage IIA	6 CVP (PR/16 mo); 4 Rituximab (CR/24 mo)	CR (64)
14	52/F	FL grade IIIa, Stage IVA	6 R-MegaCEOP (PR/10 mo); HDS (CR/6 mo)	CR (63)
1	49/F	LP, Stage IVA	6 CVP (CR/48 mo); 8 Rituximab (PR/72 mo)	PR (47)
5	52/M	FL grade I, Stage IVA	6 CVP (CR/24 mo); 4 Rituximab (PR/15 mo)	PR (12)
6	45/M	FL grade II, Stage IVA	6 R-CEOP (CR/12 mo); 4 Rituximab (PR/8 mo); HDS (CR/12 mo)	PR (7)
4	51/M	FL grade II, Stage IA	4 Rituximab (CR/24 mo); RT 30 Gy (CR/24 mo)	SD (78)
9	63/M	LP, Stage IVA	8 Rituximab (PR/16 mo); 4 CVP (PR/18 mo); 4 R-CHOP (SD/32 mo)	SD (69)
10	54/M	FL grade I, Stage IVA	8 R-CVP (CR/36 mo)	SD (68)
11	72/M	FL grade II, Stage IVB	18 mo Leukeran (CR/84 mo)	SD (10)
18	62/F	FL grade I, Stage IIIA	6 R-CVP (CR/36 mo); 4 Rituximab (CR/26 mo)	SD (52)
7	50/M	FL grade I, Stage IVA	6 CHOP (PR/12 mo); 4 Rituximab (PR/6 mo)	PD
8	56/M	FL grade II, Stage IA	3 CHOP-bleo/3 CVP (RC/16 mo) HDS (CR/24 mo); 8 Rituximab (CR/6 mo)	PD
15	72/M	LP, Stage IA	3 CHOP (PR/8 mo); Splenectomy + RT (PR/12 mo); 12 mo Leukeran (PR/7 mo); HDS (CR/12 mo); 4 Rituximab (PD/n.a.)	PD

(*Continued on the following page*)

cells and thus emphasized the ability of HS associated with γ and UVC to generate immunogenic apoptotic and necrotic bodies from NHL cell lines.

Immunogenic cell death in primary indolent NHL exposed to HS, γ-ray, and UVC ray

The results obtained in long-term NHL cell lines prompted us to investigate whether combined exposure to HS, γ, and UVC was the best way to induce immunogenic cell death in primary B-cell NHL. Because ALL constituted the cell death protocol adopted to kill indolent NHL primary cells and obtain tumor antigen cargo for patient-specific anti-lymphoma DC-based vaccines in our previous study (6), we analyzed the surface exposure of CRT and HSPs and the release of HMGB1 in treated follicular lymphoma (FL) cells isolated from four patients (Table 3; patients 1, 10, 11, and 14) before immunotherapy. After 24 hours, ALL killed over 90% of tumor cells as revealed by flow cytometry analysis of apoptosis and reached statistical significance when compared with UVC or HS (Supplementary Fig. S4A; $P = 0.049$ and $P = 0.047$). However, for each treatment condition, no significant differences were found between tumor cells from responders and nonresponders in terms of amount of cell death (Supplementary Fig. S4B). Because only a trend toward increase of CRT and HSP90 surface expression was observed in ALL compared with single agent–treated tumors (average of four FL samples; data not shown), the ability of dying FL cells to determine these parameters was assessed in samples from responders (Table 3, patients 1 and 14) and nonresponders (Table 3, patients 10 and 11), separated into two groups. The extent of CRT exposure on ALL-treated tumor cells from responders was significantly higher compared with the same samples exposed to single agents, as revealed by flow cytometry analysis of the median fluorescence intensity (MFI; Fig. 2A, white columns; $P = 0.022$, $P = 0.037$, and $P = 0.024$). ALL significantly increased CRT and HSP90 surface expression in tumor cells from responders compared with nonresponders (Fig. 2A and B, white versus gray columns, $P = 0.006$ and $P = 0.045$; Supplementary Fig. S5A and B). No statistically significant differences were found when HSP70 exposure or HMGB1 release were analyzed (data not shown). These results indicate that equally treated primary FL, with a similar clinical history, may differ in their ability to emit immunogenic signals. To determine whether the

Published OnlineFirst September 30, 2010; DOI: 10.1158/0008-5472.CAN-10-1825

Table 3. Clinical and immunologic characteristics of vaccinated patients (Cont'd)

UPN no.	Immunologic responses			Immunogenic signals in dying tumor cells			
	Post/prevaccine activated NK cell frequency*	Post/prevaccine antitumor T cells†	Post/prevaccine Treg frequency‡	% CRT$^+$	CRT MFI	% HSP90$^+$	HSP90 MFI
12	1.08	n.a.	0.82	70.87	66.10	69.74	41.30
13	1.37	n.a.	0.85	74.84	109.00	71.39	72.15
14	2.64	15§	0.16	52.91	14.80	70.50	29.00
1	0.99	3.02	0.70	43.44	7.98	62.16	43.60
5	1.11	4.84	0.74	44.83	7.80	66.31	32.25
6	1.14	4.75	1.16	73.53	78.20	59.40	45.60
4	n.a.	1.21	n.a.	58.03	22.50	21.82	6.81
9	0.62	1.01	1.18	49.15	5.26	51.50	22.80
10	1.06	1.13	1.13	31.88	17.48	35.90	22.45
11	0.57	0.89	1.43	32.21	6.50	59.44	25.10
18	1.00	0.98	1.56	51.76	18.40	39.46	25.10
7	0.86	1.05	1.57	41.92	9.07	40.82	12.40
8	0.76	0.85	0.90	41.70	8.61	23.14	7.38
15	0.84	0.91	1.33	41.67	8.15	54.30	25.10

Abbreviations: UPN, unique progressive number; LP, lymphoplasmocitoid lymphoma; CR, complete remission (44); PR, partial response (44); SD, stable disease (44); PD, progressive disease (44); CVP, cyclophosphamide, vincristine, and prednisone; R-CVP, Rituximab plus CVP; CHOP, cyclophosphamide, adryamicin, vincristine, and prednisone; R-CHOP, Rituximab plus CHOP; RT, radiotherapy; CEOP, cyclophosphamide, epiadryamicin, vincristine, and prednisone; R-CEOP, Rituximab plus CEOP; HDS, high dose sequential chemotherapy; autoBMT, autologous bone marrow transplantation; alloBMT, allogeneic bone marrow transplantation; LN, lymph nodes; BM, bone marrow; tx, therapy; n.a., not assessable.

*Post/prevaccination ratio of activated NK cell frequency measured by fluorescence-activated cell sorting (FACS) analysis of CD16 expression in $CD3^-CD56^{dim}$-gated cells (6).

†Post/prevaccination ratio of antitumor T-cell frequency at tumor site measured by IFN-γ ELISPOT assay (6).

‡Post/prevaccination ratio of Treg frequency measured by FACS analysis of $CD25^+FOXP3^+$ in $CD3^+CD4^+$-gated T cells (6).

§Post/prevaccination ratio of idiotype-specific T-cell frequency in PB measured by IFN-γ ELISPOT assay (6).

immunization efficacy of a DC-based vaccine depends on the extent of immunogenic signal exposure by dying tumor cells loaded on DCs, we searched for anti-CRT and -HSP90 antibodies in prevaccination and postvaccination serum samples. Apoptotic and necrotic DOHH-2 cells were used as target cells in Western blot analyses, because upon exposure to ALL they displayed surface CRT and HSP90 (Fig. 1A, ii and iii) as well as a significant proteome enrichment of HSP90 and Erp57, the cognate functional partner of CRT (ref. 27; Supplementary Table S1). Protein extracts were probed with biotin-conjugated immunoglobulins purified from prevaccination and postvaccination serum samples of responders (Fig. 3A, i and ii and B, i and ii; Supplementary Fig. S6) and nonresponders (Fig. 3A, iii and iv and B, iii and iv; Supplementary Fig. S6) or commercial mouse monoclonal anti-CRT (Fig. 3A, v; Supplementary Fig. S6) and anti-HSP90 (Fig. 3B, v; Supplementary Fig. S6) antibodies. Remarkably, after vaccination clinical responders showed a greater amount of circulating antibodies directed against proteins migrating at molecular weights compatible with CRT (Fig. 3A, i, ii versus v) and HSP90 (Fig. 3B, i, ii versus v) compared with nonresponders (Fig. 3A, iii, iv versus v and B, iii, iv versus v) and thus provided evidence for a positive association between tumor cell ability to expose immunogenic signals and their immunizing properties when loaded into DCs and injected into patients.

Immunogenic tumor cell death and clinical efficacy of vaccination with killed autologous NHL cell-pulsed DCs

To determine the involvement of immunogenic tumor cell death in the efficacy of DC-based active immunotherapy in indolent NHL patients, the ability of tumor cells to provide immunogenic signals on exposure to ALL was studied in all samples still available from vaccinated patients (responders, 6; nonresponders, 8) according to their outcome after vaccination (Table 3). Whereas the extent of cell death did not differ between the two groups (Fig. 4A; $P = 0.127$), CRT-positive cell percentage and MFI were significantly higher in dying tumor cells from responders compared with nonresponders, as revealed by flow cytometry (Fig. 4B, top left, $P = 0.023$ and bottom left, $P = 0.039$). Furthermore, apoptotic and necrotic bodies from tumor cells of responders expressed surface HSP90 at a higher frequency and intensity compared with those from nonresponders (Fig. 4B, top middle, $P = 0.001$ and bottom middle, $P = 0.002$); no significant differences were found when HSP70 was analyzed (Fig. 4B, top right, $P = 0.421$

Published OnlineFirst September 30, 2010; DOI: 10.1158/0008-5472.CAN-10-1825

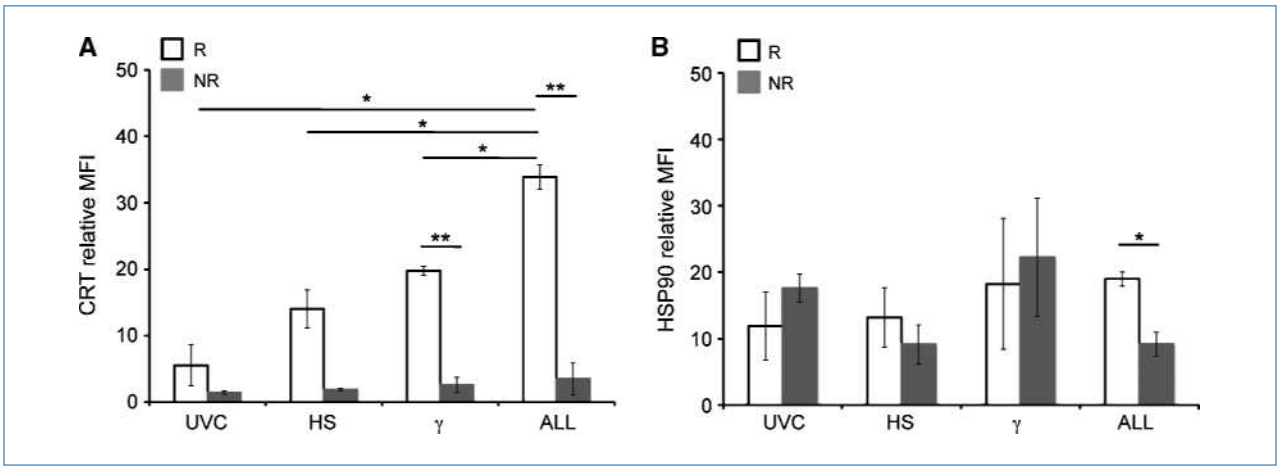

Figure 2. CRT and HSP90 expression on treated tumor cells from vaccinated patients. Flow cytometry analyses of CRT (A) and HSP90 (B) relative MFI in tumor cells from two responders (R; average patients 1 and 14, white columns) and two nonresponders (NR; average patients 10 and 11, gray columns), 24 h after exposure to UVC rays, HS, and γ irradiation as single or associated treatments (ALL). Relative MFI was calculated as the ratio between stained sample and negative control MFI of high FSC and low-SSC gated events. Significance was calculated using the two-sided Student's *t* test (*, $P \leq 0.05$; **, $P \leq 0.001$).

and bottom right, $P = 0.481$). Flow cytometry analyses of HLA class I and class II expression on dying tumor cells from responders and nonresponders revealed no significant differences (data not shown), suggesting that they shared similar antigen presentation properties. Similarly, HMGB1 release from dying tumor cells did not differ between responders and nonresponders (Fig. 4C, $P = 0.705$). We then measured the strength of the correlation between the extent of CRT and HSP90 exposure on killed autologous tumor cells used to load DCs for vaccine preparation and patient outcome after vaccination. We found a significant positive association between HSP90 surface expression in dying tumor cells and the occurrence of clinical responses (HSP90 MFI, Spearman $r = 0.8631$, $P < 0.0001$; %HSP90$^+$ cells, Spearman $r = 0.8235$, $P = 0.0003$). The frequency of tumor cells expressing surface CRT also significantly correlated with a favorable outcome after vaccination (Spearman $r = 0.6087$, $P = 0.0209$). As previously reported (6), responders showed tumor-specific T- and B-cell activation, Treg frequency reduction, and NK cell maturation, indicating a potential association between the exposure of immunogenic signals and the ability of a DC-based vaccine to induce a clinically efficient immune activation. Accordingly, clinical responses were significantly associated with NK cell maturation (Spearman $r = 0.7835$, $P = 0.0015$) and Treg frequency

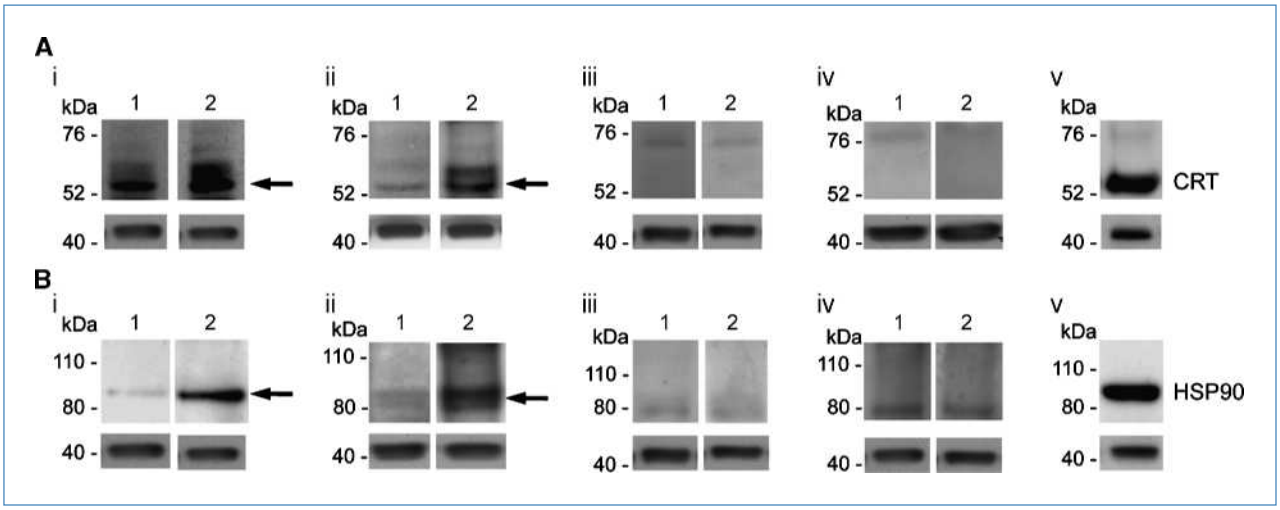

Figure 3. Vaccine-specific humoral response in clinical responders. Western blot analyses of serum-derived immunoglobulin reactivity on DOHH-2 apoptotic and necrotic body extracts. A, reactive bands obtained by probing with prevaccine (lane 1, top) or postvaccine (lane 2, top) immunoglobulins from two responders (i, patient 1; ii, patient 14) and two nonresponders (iii, patient 10; iv, patient 11) or with anti-CRT commercial monoclonal antibody (v, top). B, reactive bands obtained by probing with prevaccine (lane 1, top) or postvaccine (lane 2, top) immunoglobulins from responders (i, patient 1; ii, patient 14) and nonresponders (iii, patient 10; iv, patient 11) or with anti-HSP90 commercial monoclonal antibody (v, top). Actin protein expression is reported at the bottom of each panel as loading control. Arrows indicate specific bands for CRT and HSP90. Images were acquired on ArtixScan F1 scanner (Microtek International, Inc.) using SilverFast Launcher software (MicrotekSDK) and processed with Photoshop CS4 software (Adobe Systems, Inc.).

Published OnlineFirst September 30, 2010; DOI: 10.1158/0008-5472.CAN-10-1825

reduction (Spearman $r = -0.7835$, $P = 0.0015$), which, in turn, were found to directly correlate with the extent of CRT and HSP90 expression in the vaccine antigenic cargo (CRT MFI versus NK maturation, Pearson $r = 0.8321$, $P = 0.0004$; %CRT$^+$ cells versus NK maturation, Pearson $r = 0.7506$, $P = 0.0031$; CRT MFI versus Treg frequency reduction, Pearson $r = -0.6594$, $P = 0.0142$; HSP90 MFI versus Treg frequency reduction, Pearson $r = -0.6164$, $P = 0.0249$; %HSP90$^+$ cells versus Treg frequency reduction, Pearson $r = -0.6716$, $P = 0.0119$).

Discussion

Our study confirms in a human setting recent findings obtained in mice concerning the possibility of inducing immunogenic death in cancer cells to provide a reliable source of antigens for antitumor vaccination (1). We found that when three human NHL cell lines representing low-, intermediate- and high-grade lymphomas were treated with HS, γ, and UVC, they displayed all of the key features required to trigger a DC-mediated antitumor immune response, including the plasma membrane translocation of CRT and HSPs and the release of HMGB1 and ATP (8, 21). Because these events were enhanced when the three agents were coadministered, it is necessary to combine HS, γ, and UVC to efficiently induce an immunogenic tumor cell death. This combination was also more effective than DXR at inducing surface translocation of "eat-me" signals coupled with the release of HMGB1 and ATP. Apoptotic and necrotic tumor cell bodies generated through the exposure of primary indolent NHL cells to HS, γ, and UVC were used to pulse autologous monocyte-derived DCs and thus produce a patient-tailored vaccine. Interestingly, although displaying the same level of apoptosis, necrosis, and HMGB1 release, primary lymphoma samples from responders were better

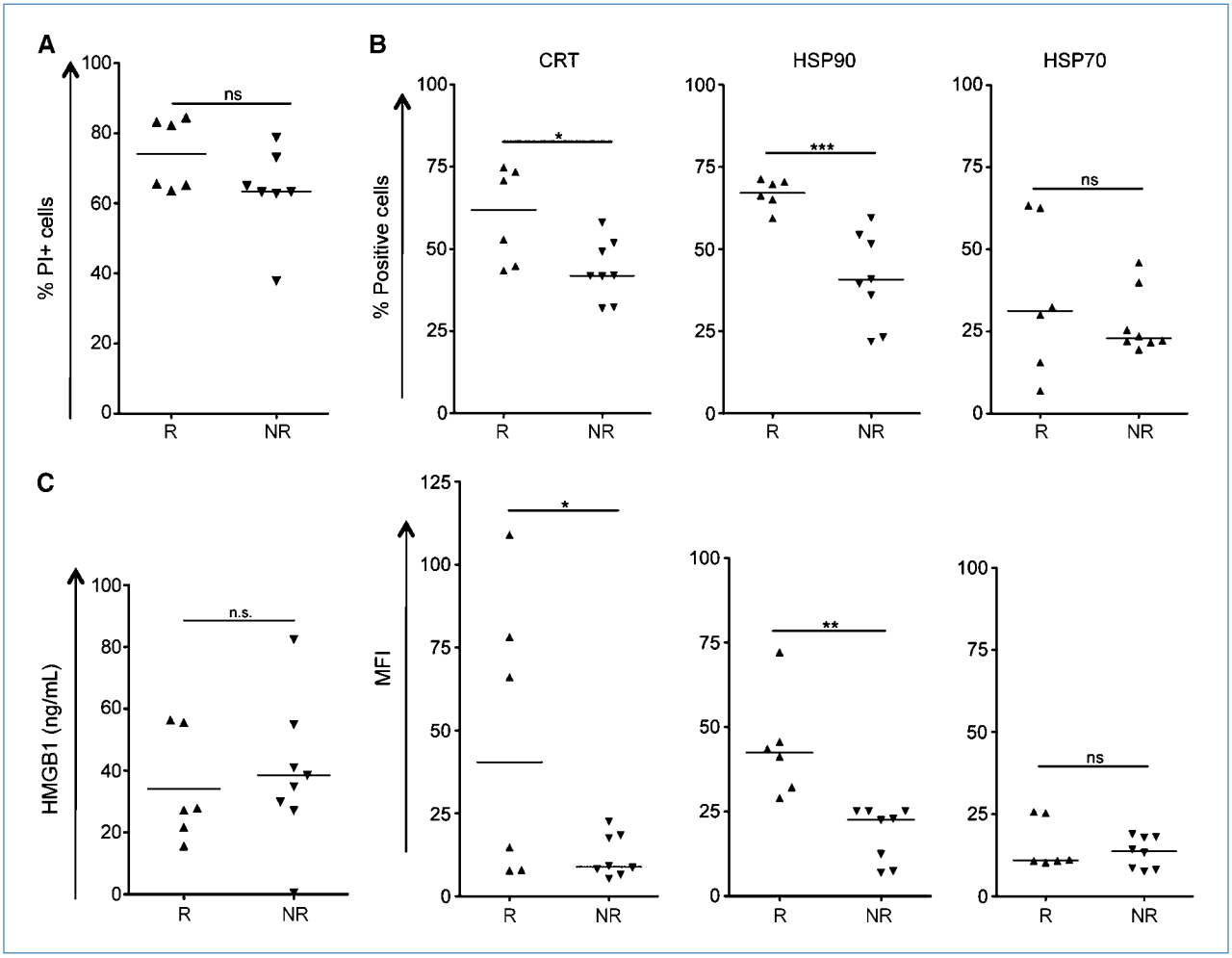

Figure 4. Lethal and immunogenic response in tumor cells from responders and nonresponders. Twenty-four hours following exposure to ALL, the ability of tumor cells from responders and nonresponders to undergo immunogenic death was assessed. Flow cytometry analyses: (A) propidium iodide$^+$ tumor cell frequency (% PI+ cells); (B) positive cell frequency (top) and MFI (bottom) for CRT (left), HSP90 (middle), and HSP70 expression (right); and (C) quantification of HMGB1 release in culture supernatant from apoptotic and necrotic tumor cells. Significance was calculated using the two-sided Student's *t* test (ns, nonsignificant difference; *, $P \leq 0.001$; **, $P \leq 0.001$; ***, $P \leq 0.0001$).

Published OnlineFirst September 30, 2010; DOI: 10.1158/0008-5472.CAN-10-1825

able to translocate CRT and HSP90 to the cell surface on exposure to the combined treatment compared with nonresponders. Remarkably, vaccination with DCs pulsed with ALL-treated autologous tumors induced the production of circulating anti-CRT and anti-HSP90 antibodies in responders, but not in nonresponders, and elicited clinical responses strongly associated with multifaceted antitumor immune activation (6). These observations in an admittedly small number of cases point to a positive correlation between the surface expression of CRT or HSP90 in dying tumor cells used as antigen cargo for a DC-based vaccine and immunologic responses associated with clinical benefit.

Our results are in line with Zitvogel and colleagues' findings that failure of one early step toward immunogenic cancer cell death was sufficient to abrogate the process (8). The lack of the CRT exposure alone, for example, may explain the hampered ability of cisplatin to induce immunogenic death in mouse colon cancer cells compared with oxaliplatin and thus reflect its limited therapeutic efficacy in colon carcinoma patients (3). Conversely, in our setting the same treatment resulted in a different exposure of "eat-me" signals in clinically comparable primary indolent NHL while reproducibly providing human NHL cell lines of different histologic grades with these immunogenic molecules. Similarly, HS exposure alone was sufficient to kill most of the cells in the three NHL cell line cultures and boost their translocation of CRT and HSP90, whereas it was less capable of eliciting the same effects in primary tumors. Alterations in the molecular pathways for chaperone trafficking (10), which render tumor cell death immunogenically silent, may confer survival advantages to B-cell NHL *in vivo* and may be selected as new immune escape mechanisms. Therefore, primary tumor cells may be less prone to undergo immunogenic cell death compared with *in vitro* established cell lines. Accordingly, the ability to downregulate CRT expression has been shown to be associated with a negative prognostic/predictive effect in colon cancer (28), neuroblastoma (29), and cervical carcinoma (30), as well as in follicular thyroid carcinoma (31). Nevertheless, our *in vitro* models consistently showed CRT and HSP90 cell surface translocation are the distinctive features induced by the combined exposure to HS, γ, and UVC. CRT involvement in immunogenic tumor cell death is also illustrated by its long investigation on account of its immunostimulatory properties, including its ability to elicit a CTL response against chaperoned antigens (13) or its own antigenic epitopes (32) as well as to induce specific autoantibodies in a variety of autoimmune diseases (33). HSP expression on the surface of dying tumor cells similarly improves their recognition by DCs (12) and increases the efficient cross-presentation of tumor-derived chaperoned antigenic peptides (14) and DC maturation (17, 34). Chaperone-rich tumor cell lysates activate NK cell effector functions in the presence of accessory cells such as DCs (35). Chaperone proteins may thus be endowed with a key role in the cross-talk between DCs and NK cells (36). By killing tumor cells, activated NK cells may render tumor antigens available for further DC cross-presentation *in vivo* (37) while inhibiting peripheral Treg conversion and directly lysing Tregs (38, 39). Regression of the tumor mass may thus result in the reestablishment of the balance between immunity and tolerance in favor of tumor immune surveillance (40). A favorable clinical outcome after vaccination, in fact, was found to be significantly associated with the extent of chaperone protein expression on apoptotic and necrotic tumor cell bodies loaded into DCs and, in turn, with NK cell activation and Treg frequency reduction (6). In keeping with the extensively described property of immunogenic tumor cell death to elicit specific T-cell responses (1, 8, 41), antitumor adaptive cellular immunity was detected at tumor site in partial responder and in PB in one complete responder, for whom a tumor-specific idiotype T-cell response was assessed (6).

All our responders showed an increased ability to translocate HSP90 compared with nonresponders, whereas three responders displayed comparable ability in CRT exposure with respect to nonresponders, meaning that at least one "eat-me" signal was sufficient to provide the proper stimuli for DC antigen uptake and activation. The considerable expression of HSP90 in vaccines administered in all responders may have compensated for the limited release of CRT in three of them.

These results delineate new ways of optimizing anticancer vaccines for the stimulation of a therapeutic antineoplastic immune response. Pulsing of DCs *ex vivo* with immunologically killed tumor cells avoids their physiologic clearance by neighboring cells before entering the late stages of the apoptotic process (19) and thus ensures optimal DC antigen uptake and activation. An explanation may thus be found for the advantages gained by using apoptotic and necrotic tumor cells to generate specific DC vaccines (42). In addition, characterization of the molecular mechanisms responsible for cell death immunogenicity may provide novel strategies to favor its occurrence during the preparation of killed tumor cell–based vaccines. Our results, indeed, showed that dying neoplastic cells, due to their impaired ability to expose CRT or HSP90, lose their immunogenic properties. Because Bcl-2 can impair CRT surface translocation (10) and its upregulation constitutes one of the hallmarks of indolent NHL, in particular FL, we investigated whether in our series Bcl-2 overexpression could explain the reduced tumor cell ability to expose CRT. However, we did not find a precise correspondence between these two features (data not shown), and the almost complete consumption of tumor cell samples for most of our vaccinated patients hampered further investigations of the mechanisms that account for these deficiencies. As shown for murine colon carcinoma and sarcoma models (11), cytotoxic agents can be combined with adjuvant compounds such as recombinant CRT or PP1/GADD34 inhibitors to enhance CRT surface expression, oligodeoxynucleotides (i.e., class A CpG), and cytokines (i.e., interleukin-1β) to boost DC engulfing, cross-presentation, and maturation, and new ways of increasing the potency of DC-based vaccination may thus be devised (9, 43).

Disclosure of Potential Conflicts of Interest

No potential conflicts of interest were disclosed.

Grant Support

Associazione Italiana per la Ricerca sul Cancro and Fondazione Michelangelo. R. Zappasodi was supported by a research fellowship from Associazione Marco Semenza.

The costs of publication of this article were defrayed in part by the payment of page charges. This article must therefore be hereby marked *advertisement* in accordance with 18 U.S.C. Section 1734 solely to indicate this fact.

Received 05/20/2010; revised 08/26/2010; accepted 09/03/2010; published OnlineFirst 09/30/2010.

References

1. Obeid M, Tesniere A, Ghiringhelli F, et al. Calreticulin exposure dictates the immunogenicity of cancer cell death. Nat Med 2007;13:54–61.
2. Casares N, Pequignot MO, Tesniere A, et al. Caspase-dependent immunogenicity of doxorubicin-induced tumor cell death. J Exp Med 2005;202:1691–701.
3. Tesniere A, Schlemmer F, Boige V, et al. Immunogenic death of colon cancer cells treated with oxaliplatin. Oncogene 2010; 29:482–91.
4. Obeid M, Panaretakis T, Joza N, et al. Calreticulin exposure is required for the immunogenicity of γ-irradiation and UVC light-induced apoptosis. Cell Death Differ 2007;14:1848–50.
5. Zitvogel L, Apetoh L, Ghiringhelli F, Kroemer G. Immunological aspects of cancer chemotherapy. Nat Rev Immunol 2008;8: 59–73.
6. Di Nicola M, Zappasodi R, Carlo-Stella C, et al. Vaccination with autologous tumor-loaded dendritic cells induces clinical and immunologic responses in indolent B-cell lymphoma patients with relapsed and measurable disease: a pilot study. Blood 2009; 113:18–27.
7. Apetoh L, Ghiringhelli F, Tesniere A, et al. Toll-like receptor 4-dependent contribution of the immune system to anticancer chemotherapy and radiotherapy. Nat Med 2007;13:1050–9.
8. Tesniere A, Apetoh L, Ghiringhelli F, et al. Immunogenic cancer cell death: a key-lock paradigm. Curr Opin Immunol 2008;20: 504–11.
9. Locher C, Rusakiewicz S, Tesniere A, et al. Witch hunt against tumor cells enhanced by dendritic cells. Ann N Y Acad Sci 2009; 1174:51–60.
10. Panaretakis T, Kepp O, Brockmeier U, et al. Mechanisms of pre-apoptotic calreticulin exposure in immunogenic cell death. EMBO J 2009;28:578–90.
11. Obeid M, Tesniere A, Panaretakis T, et al. Ecto-calreticulin in immunogenic chemotherapy. Immunol Rev 2007;220:22–34.
12. Saito K, Dai Y, Ohtsuka K. Enhanced expression of heat shock proteins in gradually dying cells and their release from necrotically dead cells. Exp Cell Res 2005;310:229–36.
13. Nair S, Wearsch PA, Mitchell DA, Wassenberg JJ, Gilboa E, Nicchitta CV. Calreticulin displays *in vivo* peptide-binding activity and can elicit CTL responses against bound peptides. J Immunol 1999;162:6426–32.
14. Srivastava PK. Immunotherapy for human cancer using heat shock protein-peptide complexes. Curr Oncol Rep 2005;7:104–8.
15. Binder RJ, Srivastava PK. Peptides chaperoned by heat-shock proteins are a necessary and sufficient source of antigen in the cross-priming of CD8+ T cells. Nat Immunol 2005;6:593–9.
16. Feng H, Zeng Y, Whitesell L, Katsanis E. Stressed apoptotic tumor cells express heat shock proteins and elicit tumor-specific immunity. Blood 2001;97:3505–12.
17. Somersan S, Larsson M, Fonteneau JF, Basu S, Srivastava P, Bhardwaj N. Primary tumor tissue lysates are enriched in heat shock proteins and induce the maturation of human dendritic cells. J Immunol 2001;167:4844–52.
18. Gardai SJ, McPhillips KA, Frasch SC, et al. Cell-surface calreticulin initiates clearance of viable or apoptotic cells through trans-activation of LRP on the phagocyte. Cell 2005;123:321–34.
19. Savill J, Dransfield I, Gregory C, Haslett C. A blast from the past: clearance of apoptotic cells regulates immune responses. Nat Rev Immunol 2002;2:965–75.
20. Ghiringhelli F, Apetoh L, Tesniere A, et al. Activation of the NLRP3 inflammasome in dendritic cells induces IL-1β-dependent adaptive immunity against tumors. Nat Med 2009;15:1170–8.
21. Aymeric L, Apetoh L, Ghiringhelli F, et al. Tumor cell death and ATP release prime dendritic cells and efficient anticancer immunity. Cancer Res 2010;70:855–8.
22. Scaffidi P, Misteli T, Bianchi ME. Release of chromatin protein HMGB1 by necrotic cells triggers inflammation. Nature 2002;418: 191–5.
23. Di Nicola M, Napoli S, Anichini A, et al. Dendritic cell viability is decreased after phagocytosis of apoptotic tumor cells induced by staurosporine or vaccinia virus infection. Haematologica 2003;88: 1396–404.
24. Zappasodi R, Di Nicola M, Carlo-Stella C, et al. The effect of artificial antigen-presenting cells with preclustered anti-CD28/-CD3/-LFA-1 monoclonal antibodies on the induction of *ex vivo* expansion of functional human antitumor T cells. Haematologica 2008;93:1523–34.
25. Pupa SM, Argraves WS, Forti S, et al. Immunological and pathobiological roles of fibulin-1 in breast cancer. Oncogene 2004;23: 2153–60.
26. Gorla L, Mondellini P, Cuccuru G, et al. Proteomics study of medullary thyroid carcinomas expressing RET germ-line mutations: identification of new signaling elements. Mol Carcinog 2009;48:220–31.
27. Panaretakis T, Joza N, Modjtahedi N, et al. The co-translocation of ERp57 and calreticulin determines the immunogenicity of cell death. Cell Death Differ 2008;15:1499–509.
28. Toquet C, Jarry A, Bou-Hanna C, et al. Altered Calreticulin expression in human colon cancer: maintenance of Calreticulin expression is associated with mucinous differentiation. Oncol Rep 2007;17: 1101–7.
29. Hsu WM, Hsieh FJ, Jeng YM, et al. Calreticulin expression in neuroblastoma-a novel independent prognostic factor. Ann Oncol 2005;16:314–21.
30. Mehta AM, Jordanova ES, Kenter GG, Ferrone S, Fleuren GJ. Association of antigen processing machinery and HLA class I defects with clinicopathological outcome in cervical carcinoma. Cancer Immunol Immunother 2008;57:197–206.
31. Netea-Maier RT, Hunsucker SW, Hoevenaars BM, et al. Discovery and validation of protein abundance differences between follicular thyroid neoplasms. Cancer Res 2008;68:1572–80.
32. Lieu TS, Newkirk MM, Capra JD, Sontheimer RD. Molecular characterization of human Ro/SS-A antigen. Amino terminal sequence of the protein moiety of human Ro/SS-A antigen and immunological activity of a corresponding synthetic peptide. J Clin Invest 1988;82: 96–101.
33. Eggleton P, Ward FJ, Johnson S, et al. Fine specificity of autoantibodies to calreticulin: epitope mapping and characterization. Clin Exp Immunol 2000;120:384–91.
34. Spisek R, Charalambous A, Mazumder A, Vesole DH, Jagannath S, Dhodapkar MV. Bortezomib enhances dendritic cell (DC)-mediated induction of immunity to human myeloma via exposure of cell surface heat shock protein 90 on dying tumor cells: therapeutic implications. Blood 2007;109:4839–45.
35. Zeng Y, Chen X, Larmonier N, et al. Natural killer cells play a key role in the antitumor immunity generated by chaperone-rich cell lysate vaccination. Int J Cancer 2006;119:2624–31.
36. Zeng Y, Feng H, Graner MW, Katsanis E. Tumor-derived,

Published OnlineFirst September 30, 2010; DOI: 10.1158/0008-5472.CAN-10-1825

chaperone-rich cell lysate activates dendritic cells and elicits potent antitumor immunity. Blood 2003;101:4485–91.
37. Munz C, Steinman RM, Fujii S. Dendritic cell maturation by innate lymphocytes: coordinated stimulation of innate and adaptive immunity. J Exp Med 2005;202:203–7.
38. Brillard E, Pallandre JR, Chalmers D, et al. Natural killer cells prevent CD28-mediated Foxp3 transcription in CD4+CD25- T lymphocytes. Exp Hematol 2007;35:416–25.
39. Roy S, Barnes PF, Garg A, Wu S, Cosman D, Vankayalapati R. NK cells lyse T regulatory cells that expand in response to an intracellular pathogen. J Immunol 2008;180:1729–36.
40. Yang ZZ, Novak AJ, Stenson MJ, Witzig TE, Ansell SM. Intratumoral CD4+CD25+ regulatory T-cell-mediated suppression of infiltrating CD4+ T cells in B-cell non-Hodgkin lymphoma. Blood 2006;107:3639–46.
41. Tesniere A, Panaretakis T, Kepp O, et al. Molecular characteristics of immunogenic cancer cell death. Cell Death Differ 2008;15:3–12.
42. Strome SE, Voss S, Wilcox R, et al. Strategies for antigen loading of dendritic cells to enhance the antitumor immune response. Cancer Res 2002;62:1884–9.
43. Zitvogel L, Apetoh L, Ghiringhelli F, Andre F, Tesniere A, Kroemer G. The anticancer immune response: indispensable for therapeutic success? J Clin Invest 2008;118:1991–2001.
44. Cheson BD, Pfistner B, Juweid ME, et al. Revised response criteria for malignant lymphoma. J Clin Oncol 2007;25:579–86.

Published OnlineFirst September 30, 2010; DOI: 10.1158/0008-5472.CAN-10-1825

AACR American Association for Cancer Research

Cancer Research

The Journal of Cancer Research (1916–1930) | The American Journal of Cancer (1931–1940)

Improved Clinical Outcome in Indolent B-Cell Lymphoma Patients Vaccinated with Autologous Tumor Cells Experiencing Immunogenic Death

Roberta Zappasodi, Serenella M. Pupa, Gaia C. Ghedini, et al.

Cancer Res 2010;70:9062-9072. Published OnlineFirst September 30, 2010.